# 7: MODELLING THE THERMAL BEHAVIOUR OF FABRIC MEMBRANES.

## 7:1.    INTRODUCTION.

In this chapter the development of a model which allowed the thermal behaviour of fabric membranes to be predicted is described. This model had two fundamental aims:-

- To provide a tool which may be used to investigate the thermal behaviour of fabric membranes.
- To provide a means for generating the boundary information necessary in order to predict the thermal behaviour of spaces enclosed by fabric membranes.

Because of the unusually responsive thermal behaviour of fabric membranes it was considered necessary to develop an entirely new model specifically for this purpose, based on only the most appropriate theoretical techniques. This model was substantiated with the properties information described in Chapter 6, and validated using the behavioural data presented in Chapter 5.

A complete listing of the model code is presented in Appendix 2 at the end of this thesis.

## 7:2.    GENERAL DESCRIPTION OF A MODEL DEVELOPED IN ORDER TO PREDICT THE THERMAL BEHAVIOUR OF FABRIC MEMBRANES.

### 7:2.1    The Purpose of the Boundary Model.

In order to generate information with which the thermal behaviour of spaces enclosed by fabric membranes might be determined, the model was required to predict two basic behavioural parameters which were previously identified in Chapter 5:-

- The quantity of solar radiation directed into a space by the fabric membrane enclosing it.
- The internal surface temperature of that fabric membrane.

The first of these parameters could be composed of both the external solar radiation transmitted through the membrane, and the internal solar radiation reflected back into the enclosure from the internal surface of the membrane. It was necessary to predict both of these quantities as the spatial model described in Chapter 9 had no facility for simulating the internal reflected component of solar radiation.

The second parameter allowed the heat exchange by long wave infra red radiation and convection between the membrane and the space it enclosed  to be determined.

7:2.2 **Simplifications Made in Order to Predict the Thermal Behaviour of Fabric Membranes.**

Given that the solar optical properties of the membrane samples had already been determined (see Chapter 6), it was considered that it would be relatively simple to predict the quantity of solar radiation directed into the enclosed space.

Predicting the internal surface temperature of a fabric membrane however was likely to be considerably more complex, and so a series of simplifications were made in order to make the thermal situation that was being investigated more manageable.

• The problem area was first limited to a finite domain within which both environmental conditions and material properties could be considered to be uniform. This involved breaking down the complex doubly curved geometry typical of fabric membrane envelopes into a series of panels or '*finite elements*' across which variations in behaviour could be considered insignificant.

• Secondly, in order to avoid having to consider all the notional panels of a membrane envelope simultaneously, each panel was considered to behave independently of the others. Because of the very small cross section of fabric membranes and the insignificant behavioural differences likely to build up between adjacent panels of a progressively undulating membrane envelope, this was considered to be a reasonable assumption.

For the purposes of validating the model with the data presented in Chapter 5, both of these assumptions were realistic. The test cell membrane samples were all single, isolated, flat panels.

• The third more unusual assumption however , as previously discussed in Chapter 5, was that thin fabric membranes have such low thermal mass compared to their surface area that it may be assumed they insufficient thermal capacity to significantly affect their thermal behaviour.

Accepting this assumption meant that membrane panels could be considered to react instantly and completely to changes in their thermal environment. If the *equilibrium temperature* of a membrane panel (that temperature at which it is neither losing or gaining heat to its surroundings) was tracked over time therefore, this should show a good approximation of its transient thermal behaviour. This assumption will be discussed further throughout the rest of this chapter.

7:2.3 **The Format of the Model Developed in Order to Predict the Thermal Behaviour of Fabric Membranes.**

The basic model was developed in a spread sheet format. Whilst this user friendly approach incurred a considerable computational overhead, it had the advantage of allowing the easy visualisation of calculation paths, and this proved invaluable during the course of its development.

It consists of six basic spreadsheets which are listed below, and the relationship between these spreadsheets is illustrated schematically in *Figure 7:3.2.*

- Data Base of Membrane Properties.
- Data Base of Site Descriptions.
- Time Series Data Base of Environmental Conditions.
- Control Programme.
- Solar Model.
- Heat Transfer Model.

*Figure 7:2.3 Schematic Illustration of the Model Format.*
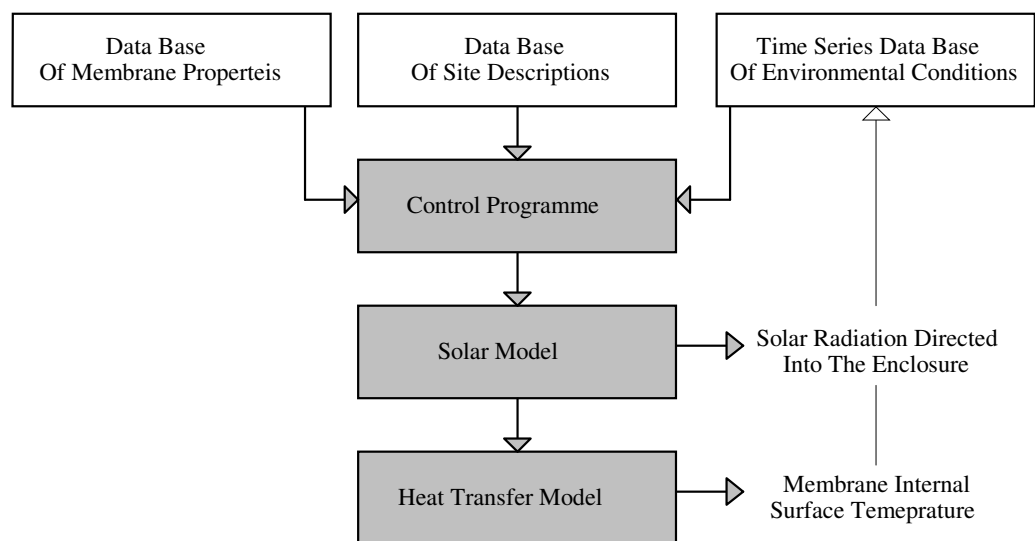


The purpose of these six components is described below.

- *Data Base of Membrane Properties.*
  This data base contains information regarding those properties which were considered to significantly influence the thermal behaviour of the fabric membranes being investigated. The selection of the properties included in this data base was explained in Chapter 5 and the measurement of those properties which could not be obtained from membrane manufacturers was described in Chapter 6.

The properties specified were:-

- Core thermal conductivity (excluding surface resistances).
- Near normal solar transmittance.
- Near normal solar reflectance.
- Near normal solar absorptance.
- Diffuse solar transmittance.
- Diffuse solar reflectance.
- Diffuse solar absorptance.
- External surface near normal emissivity.
- Internal surface near normal emissivity.

The properties of the range of membranes investigated in the thesis are permanently listed in this data base. The model user merely has to select a membrane type and the relevant properties are then automatically transferred to the *Solar Model* and *Heat Transfer Model*.

- *Data Base of Site Descriptions.*
  This data base contains information relating to all those permanent site *features* which it was considered could significantly affect the thermal behaviour of the membrane panel being investigated.

The parameters specified in this spread sheet are:-

- The characteristic surface area of the membrane envelope.
- The characteristic perimeter length of the membrane envelope.
- The characteristic height of the membrane envelope.
- The average solar reflectance of objects facing the internal surface of the membrane.
- The average emissivity of objects facing the internal surface of the membrane.
- The membrane panel longitude.
- The membrane panel latitude.
- The membrane panel elevation.
- The average obstruction angle of external surrounding objects above the horizon.
- The average solar reflectivity of objects facing the external surface of the membrane.

Again, the properties of all the sites investigated during the course of this research are listed permanently in this data base. The model user therefore merely has to select the appropriate site and its thermal description is then automatically transferred to the *Solar Model* and *Heat Transfer Model*.

- *Time Series Data Base of Environmental Conditions.*

  This time series data base specifies the thermal *state* of the internal and external environments surrounding the membrane panel for each instant to be investigated.

  The conditions specified in this spread sheet are:-

  - The date and time.
  - The average internal air speed caused by any active ventilation systems.
  - The average temperature of objects facing the inside surface of the membrane.
  - The characteristic air temperature within the enclosed space.
  - The intensity of external horizontal global solar radiation.
  - The external air temperature.
  - The external free stream wind speed.
  - The external free stream wind direction.
  - The azimuth of the membrane panel.
  - The inclination of the membrane panel.

  This data is listed in a time series format such that the line of data at the top of the series represents the active conditions. The active line is read by the calculations worksheet in order to quantify environmental conditions, and then as progressive time steps are solved that line is removed and the next time step becomes active.

- *Control Programme.*

  The *Control Programme* initiates the sequence of operations undertaken by the model once the problem has been specified, in order to solve the model equations and control the progression of data from one time step to the next. Because of the importance of this process, the *Control Programme* is described in detail in Section 4 of this chapter.

- *Solar Model.*

  The *Solar Model* contains the theory with which the intensity of solar radiation directed into the enclosed space by the membrane panel can be determined. The information produced by this part of the model also allowed the quantity of solar radiation absorbed by the membrane to be calculated in order that its internal surface temperature could be predicted.

  The *Solar Model* developed into something more complex than may have been expected because of the requirements of the spatial investigations described in the second part of this thesis. Although the test cell discussed in Chapter 5 was designed specifically in order that the intensity of solar radiation incident upon the membrane sample was known, this was not the case in the programme of site monitoring described in Chapter 8. It was only

feasible to set up a simple meteorological station close to the buildings investigated, and this did not allow the varying intensities of solar radiation incident upon the doubly curved membrane envelopes to be monitored.

As it was only really practical to record horizontal global solar radiation, a method was required which allowed the intensity of solar radiation incident upon a surface of known orientation to be predicted. These predictions involve three basic stages:-

- Calculation of the angle of incidence of direct beam solar radiation incident on the external surface of the membrane.
- Calculation of the composition of solar radiation incident on the external surface of the membrane.
- Calculation of the composition of solar radiation incident on the internal surface of the membrane.

Because of the great importance of these parts of the *Solar Model* on the accuracy of the overall membrane model, the specific methods adopted by each of the them is described in detail in the section 3 of this chapter.

- *Heat Transfer Model.*
  This spread sheet model contains the theoretical calculations which are used in order to predict the internal surface temperature of the membrane panel being investigated. Because of the low thermal capacity of fabric membranes, this only involves calculating the net heat transfer between the membrane and its surroundings at any instant and then using this to predict its *equilibrium temperature*.

The net heat transfer between the membrane panel and its surroundings is calculated based upon five basic sub routines:-

- Calculation of the external surface long wave infra red radiation heat transfer.
- Calculation of the internal surface long wave infra red radiation heat transfer.
- Calculation of the external surface convection heat transfer.
- Calculation of the internal surface convection heat transfer.
- Calculation of the membrane core behaviour.

Because of the importance of these five components of the model, the specific methods adopted by each of them is described in detail in the Section 4 of this chapter.

## 7:3. DESCRIPTION OF THE SOLAR MODEL.

### 7:3.1 Introduction.

The purpose of the solar model is to determine the intensity of solar radiation directed into the enclosure by the membrane panel being investigated. These calculations can also be used to provide information with which the quantity of solar radiation absorbed by the membrane may be calculated.

The primary function of the solar model is to determine the intensity of solar radiation incident upon the internal and external surfaces of the membrane panel given that the intensity of horizontal global solar radiation is known. This is done according to three basic processes:-

- Calculation of the angle of incidence of direct beam solar radiation incident on the external surface of the membrane.
- Calculation of the composition of solar radiation incident on the external surface of the membrane.
- Calculation of the composition of solar radiation incident on the internal surface of the membrane.

The parameters predicted by these three processes are illustrated schematically by *Figure 7:3.1* below.

*Figure 7:3.1 Diagram to Illustrate the Parameters Predicted by Solar Model.*
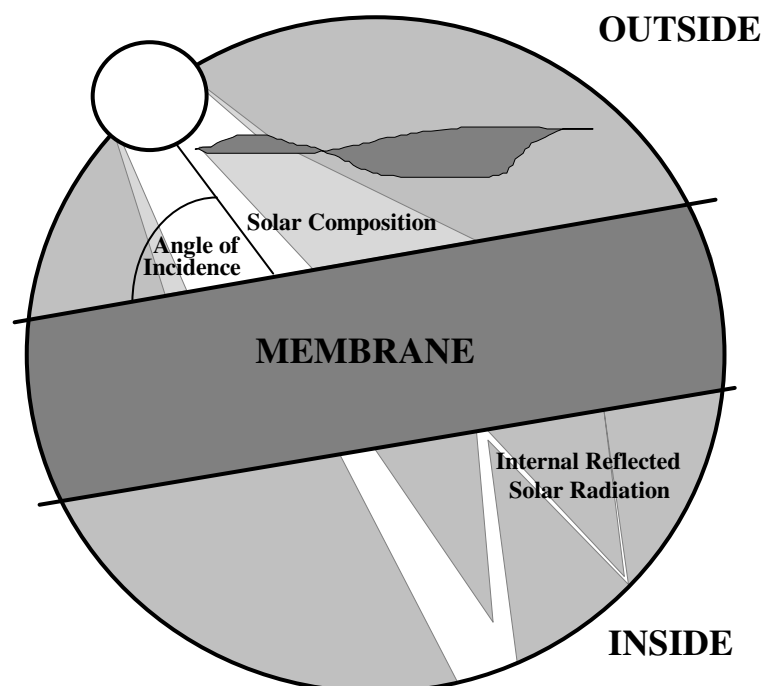
7:3.2 **Calculation of the Angle of Incidence of Direct Beam Solar Radiation Incident on the External Surface of the Membrane.**

These calculations are carried out in order to predict the position of the sun relative to the membrane panel so that the intensity and direction of solar radiation incident upon it can be predicted. This first requires that the position of the sun within the sky is determined, and this is described in terms of *Solar Altitude* and *Solar Azimuth.*

*Figure 7:3.2 Diagram to Illustrate Solar Azimuth and Altitude.*
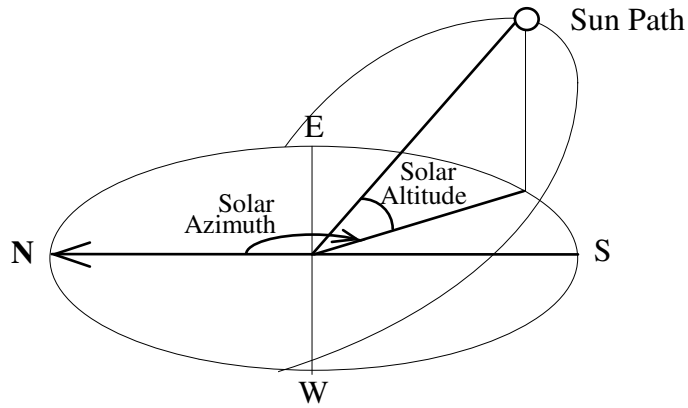


The process for determining the *Solar Altitude* and *Solar Azimuth* is well established and this is described below.

- Firstly, the observed *local time* is converted into *Greenwich Mean Time* (GMT) by taking account of any daylight saving hours such as British Summer Time. This conversion can result in the observed time being moved into the preceding or following day, and so the date is corrected accordingly and converted into a *day number* (Y), for which January 1st = 1, January 2nd = 2 etc.

- Given the *site longitude*, the *solar time* can be determined by correcting the GMT according to the *equation of time. Solar time* describes the apparent progress of the sun as it travels across the sky, returning to cross the same local meridian after a full solar day. This takes account of the elliptical orbit of the earth about the sun, and the inclination of the earth relative to the plane of this ellipse.

*day angle* $(\theta_y) = 360 \times Y / 365.25$ [1]

*equation of time* $(E_{ot}) = -0.128 \sin(\theta_y - 2.8) - 0.165 \sin(2\theta_y + 19.7)$ [2]

*solar time* $(S_t) = GMT + [(longitude - local\ time\ reference\ longitude) / 15] + E_{ot}$ [3]

- It is then possible to calculate the *hour angle* ($\theta_h$) which is an angular expression of *solar time* relative to the *longitude* of the site.

  $$\theta_h = 15 \times \mid 12 - S_t \mid \tag{[4]}$$

- Given the *day number*, the *solar declination* (d) can be determined. *Solar declination* describes the angle that a line drawn between the centre of the earth and the centre of the sun would subtend with the plane of the earth's equator.

  $$d = 23.45 \sin ( 280.1 + 0.9863Y ) \tag{[5]}$$

- From the *solar declination*, the *hour angle* and the *site latitude* ($\phi$), the *solar azimuth* ($A_Z$) and *solar altitude* ($A_S$) can be calculated.

  $$A_S = A\sin [ \cos (\phi) \cos (d) \cos ( \theta_h ) + \sin (\phi) \sin (d) ] \tag{[6]}$$

  $$A_Z = A\sin [ \cos (d) \sin (\theta_h) / \cos (A_S) ] \tag{[7]}$$

  When the azimuth ($A_W$) and inclination ($\beta$) of the membrane panel are known, the angle of incidence (i) of direct beam solar radiation striking the external surface of the  membrane can be calculated.

  $$i = A\cos ( \cos (A_S) \cos (A_Z - A_W) \sin (\beta) + \sin (A_S) \cos (\beta) \tag{[8]}$$

  This simple situation is complicated by the scattering affect of the earth's atmosphere, which means that whilst some of the solar radiation incident upon the membrane surface will be *direct beam*, a proportion will also be *diffuse*. To determine the actual angular nature and intensity of solar radiation incident upon the external surface of the membrane panel therefore, the composition of that solar radiation has to be calculated.

## 7:3.3 Calculation of the Composition of Solar Radiation Incident on the External Surface of the Membrane.

As solar radiation passes through the atmosphere so its path is obstructed by small particles such as the constituent molecules of air (in particular ozone), water vapour, clouds, pollution and so on. These particles progressively absorb and scatter solar radiation, and as a result terrestrial insolation tends to be at least partially diffuse.

There are a number of ways of determining the extent of this scattering effect however in order to satisfy the specific requirements of this research, a new solar model was developed, constructed from the most appropriate and realistic parts of several existing models. The procedure adopted by this model involves estimating the intensity of *horizontal global solar radiation* that there would be if the sky were entirely '*clear*' and then comparing this with the monitored value in order to predict the *cloudiness* of the sky.

The extent to which a *clear sky* will scatter the solar radiation which passes through it can be described by a clearness index ($K_t$).

$$K_t = I_{dn} / I_{et}$$
[9]

where $I_{dn}$ represents the intensity of *normal direct beam solar radiation* incident on the earth's surface, and $I_{et}$ the intensity of *normal extraterrestrial solar radiation*. $K_t$ can be estimated based on the *air mass* through which solar radiation has to pass in order to reach the earth's surface, the *turbidity* of that air mass, and the quantity of precipitable water which it contains. This process is described below.

- The *solar constant* ($I_{sc}$) describes the annual mean solar radiation incident on an extraterrestrial surface perpendicular to a line drawn between the earth and the sun, and this is taken to be $1377 W/m^2$ [10]. This mean value can be corrected based on the *year day number* (Y) to account for the elliptical orbit of the sun about the earth.

*Corrected solar constant* $(I_{sc1}) = I_{sc} \{1 + 0.033 \cos [(360 - Y)/370]\}$
[11]

- Given that the *solar altitude* ($A_s$) and *membrane elevation* (h) are known , it is possible to estimate the *air mass* (m) through which this solar radiation has to pass in order to reach the membrane:-

if $A_s < 10$

$$m = \exp[h(-0.0017h - 0.1174)] \times \exp\left\{3.67985 + \sum_{i=1}^{6} e_i \left[\sin(A_s)\right]^i\right\}$$

|   | 1 | 2 | 3 | 4 | 5 | 6 |
|---|---|---|---|---|---|---|
| e | -24.4465 | 154.017 | -742.181 | 2263.36 | -3804.89 | 2261.05 |

or if $A_s \geq 10$     $m = \exp [h (-0.0017h - 0.1174)] / \sin A_s$
[12]

- It proved impractical to measure the *turbidity* ($T_L$) of the air mass, and so typical monthly values for the sites investigated during the course of this research were taken from statistical analysis of existing recorded data[13].

These values can then be adjusted to account for the actual altitude of the sun to give a *corrected turbidity* $T_L(A_S)$.

$$T_L(A_S) = T_L - 0.85 + 2.25 \sin (A_S) + 1.11 \sin^2 (A_S)$$

or if $T_L < 2.5$:-    $T_L(A_S) = T_L - [0.85 - 2.25 \sin(A_S) + 1.11 \sin^2(A_S)] (T_L - 1) / 1.5$     [14]

For simplicity, this value is then converted into a turbidity coefficient $T_c$.

$$T_c = -0.128 + 0.07 T_L(A_S)$$     [15]

- The likely *precipitable water content* of the atmosphere can also be estimated based on statistical analysis of observed values.

$$W = 10.44 + \sum_{i=1}^{3} \left[ c_i \cos(wi) + d_i \cos(wi) \right] \qquad \text{where } w = 2\pi Y / 366 \qquad [16]$$

|   | i1 | i2 | i3 |
|---|---|---|---|
| c | -6.468 | 1.056 | -0.128 |
| d | -3.492 | 2.049 | 0.579 |

- It is then possible to estimate the theoretical scattering and attenuation of extraterrestrial solar radiation as it passes through the atmosphere assuming there is no cloud cover.

$$K_t = \exp\left[ \sum_{i=0}^{3} \left( \sum_{j=0}^{2} b_{ij} W^j \right) m^i \right] \times \exp(-T_c m)$$     [17]

| b | i0 | i1 | i2 | i3 |
|---|---|---|---|---|
| j0 | -0.12964 | -0.0642111 | -0.0046883 | 0.000844097 |
| j1 | 0.00412828 | -0.00801046 | -0.00220414 | -0.000191442 |
| j2 | -0.0112096 | 0.0153069 | -0.00429818 | 0.00374176 |

From this the intensity of *clear sky direct beam normal solar radiation* can be determined.

$$I_{dnl} = I_{et} \times K_t$$

And so the intensity of *clear sky horizontal direct beam solar radiation* can be calculated.

$$I_{dhl} = I_{dnl} \sin (A_S)$$

- Parmalee has suggested that there is a direct relationship between the intensity of *theoretical clear sky direct beam normal solar radiation*, and the intensity of *theoretical clear sky horizontal diffuse solar radiation* ($I_{fhl}$)[18].

$$I_{fhl} = 2 + \left[ \sum_{i=1}^{7} f_i \left( \frac{A_s}{10} \right)^i \right] \times \left[ 1 + 0.033 \cos \left( \frac{360 - Y}{370} \right) \right] - \left[ 10^{-3} \sum_{i=0}^{5} g_i \left( \frac{A_s}{10} \right)^i \right] \times I_{dnl} \sin(A_s)$$

|   | i0 | i1 | i2 | i3 | i4 | i5 | i6 | i7 |
|---|----|----|----|----|----|----|----|----|
| f |    | 47.382 | 29.671 | -15.8621 | 4.3463 | -0.57764 | 0.03472 | -0.00736 |
| g | 297 | 1.8313 | -3.7082 | 4.1233 | 0.6409 | 0.02855 |  |  |

And so the *theoretical clear sky horizontal global solar radiation* (G) can be determined:-

$G = I_{dh1} + I_{fhl}$

- Szolokay proposed that this *theoretical clear sky horizontal global solar radiation* can be used to estimate a *cloudiness index* (N), where N is equal to the *measured horizontal global solar radiation* (H) divided by the *theoretical clear sky horizontal global solar radiation* (G) [19].

$N = H / G$

Given N it is then possible to calculate the intensity of the *cloudy sky horizontal diffuse solar radiation* (D).

if $0 < N \leq 0.4$,     D = 0.94 G
if $0.4 < N \leq 1$     D = [( 1.29 - 1.19 N ) / ( 1 - 0.334 N )] G
if $N > 1$     D = 0.15 G     [20]

- As the position of the sun relative to the membrane panel has already been determined, and the orientation of the membrane panel is known, it is then possible to calculate the intensity of *sky diffuse solar radiation* ($I_{sf}$) and the intensity of *direct beam solar radiation* ($I_d$) incident upon the external surface of the membrane panel.

$I_d = ( G - D ) \times \cos (i)$     [21]

$I_{sf} = D[0.5( 1+\cos\beta )][1+[1-( D^2/ G^2 )] \sin^3(\beta/2)\}[1+[1-( D^2/ G^2 )] \sin^3(90 - A_s)\}$     [22]

An addition must then be made to this value in order to account for solar radiation incident upon the external surface of the membrane as a result of reflections from surrounding objects. This reflected solar radiation is considered to be entirely diffuse, and so the intensity incident upon the membrane panel can be determined from the relative view that the membrane has of surrounding surfaces.

To simplify the situation, external surfaces are categorised as *ground*, or *obstruction* surfaces. The material composition of these surroundings can be estimated by the user based on a list of commonly occurring materials included in the *Site Descriptions* spread sheet, for which the angular solar reflectance is known. The *view factors* that the membrane had of those surfaces can then determined.

- The *ground i*s assumed to be flat, an assumption which was appropriate for all the sites investigated in the course of this research. The *ground view factor* therefore is taken to be equal to the inclination of the membrane divided by the full 180$^o$ available within hemisphere surrounding the external surface of the membrane.

- Surrounding *obstructions* are considered on average to be vertical and facing in the opposite direction to the membrane azimuth. The average angle between the ground and the top of the surrounding obstructions is input by the user as an obstruction *view angle*, and the *obstruction view factor* can then be calculated as equal to the *view angle* divided by the full 180$^o$ of the external hemisphere.

- The remainder of the hemisphere can then be assumed to be open to the *sky*.

*Figure 7:3.3 Diagram to Illustrate the External Hemispherical View Factors.*
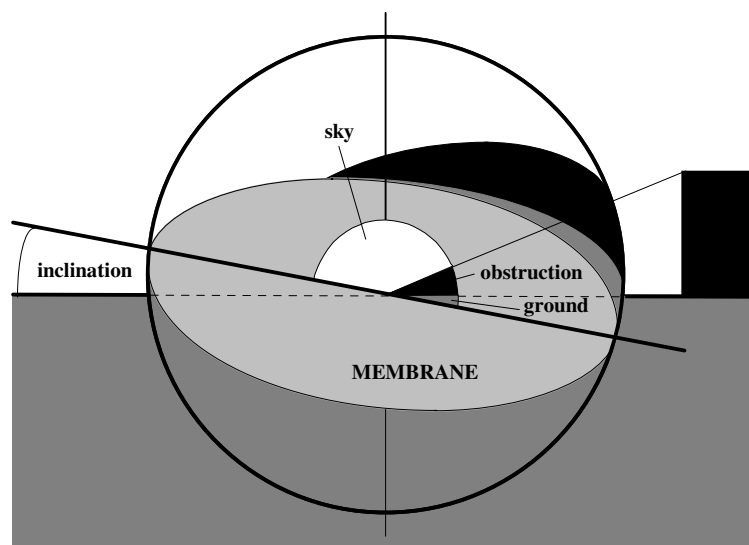
The angle of incidence and intensity of solar radiation striking these surfaces is then calculated using the same technique as was previously described for determining the angle of incidence and intensity of solar radiation striking the membrane panel. Based on their angular solar reflectance, and relative *view factors*, it is then possible to determine the intensity of reflected solar radiation incident upon the external surface of the membrane.

Adding this value to the *incident sky diffuse solar radiation* ($I_{sf}$) gives the *total incident diffuse solar radiation* ($I_f$).

- From the approximations of the angular solar optical properties [$\rho(i)$, $\tau(i)$, $\alpha(i)$] and diffuse solar optical properties [$\rho(f)$, $\tau(f)$, $\alpha(f)$]of the membrane samples, described in the previous chapter, it is then possible to predict the total external incident solar radiation transmitted, reflected and absorbed by the membrane ($q\rho_{(ext)}$, $q\tau_{(ext)}$, $q\alpha_{(ext)}$).

$$q\rho_i = I_d \times \rho(i)$$
$$q\rho_f = I_f \times \rho(f)$$
and $\quad q\rho_{(ext)} = q\rho_f + q\rho_i$

$$q\tau_i = I_d \times \tau(i)$$
$$q\tau_f = I_f \times \tau(f)$$
and $\quad q\tau_{(ext)} = q\tau_f + q\tau_i$

$$q\alpha_i = I_d \times \alpha(i)$$
$$q\alpha_f = I_f \times \alpha(f)$$
and $\quad q\alpha_{(ext)} = q\alpha_f + q\alpha_i$

7:3.4 **Calculation of the Intensity of Solar Radiation Incident on the Internal Surface of the Membrane.**

These calculations are carried out in order to determine the quantity of solar radiation transmitted through the membrane envelope which after multiple reflections within the enclosure may then be incident on the internal surface of the membrane panel.

Because of the curved nature of membrane envelopes, the solar radiation transmitted through the specific panel being modelled may not be representative of the average solar radiation passing through the membrane envelope as a whole. As the curvatures of membrane envelopes tend to balance however, it is assumed by the model that the solar radiation transmitted through a flat horizontal membrane will be representative of the average behaviour of the entire envelope.

Because of the varying angles of incidence of solar radiation incident upon doubly curved membranes, diffuse solar optical properties are considered to be representative of this *average* membrane panel. The total solar radiation transmitted through the membrane is then calculated as the *measured horizontal global solar radiation* (H) multiplied by the *membrane diffuse solar transmittance* ($\tau(f)$).

It is assumed that the representative flat membrane forms an infinite plane parallel to and facing towards an infinite plane whose solar optical properties are representative of the objects facing its internal surface. This means that all solar radiation transmitted through the membrane is incident upon this representative surface and then subsequently reflects back to the membrane.

The transmitted solar radiation is then assumed to follow a '*transient*' path whereby as a result of successive reflections between the membrane and the interior, it is progressively absorbed, until following multiple reflections the remaining solar radiation is negligible. It is generally found that the remaining internal solar radiation is insignificant after 10 internal reflections. Solar absorptance, transmittance and reflectance are calculated at each reflection, based on the diffuse properties of the membrane panel, and the sum of these values allows the total solar radiation absorbed, reflected and transmitted by its internal surface to be calculated ($q_{\alpha(int)}$, $q_{\rho(int)}$, $q_{\tau(int)}$).

NB  This is not the same as the value used to predict the solar intensity within the membrane enclosures simulated in Chapter 9, nor is it the same as the value used to predict the intensity of solar radiation incident on the internal surface of the test cell samples, both of which were calculated based on actual membrane orientations and angular properties.

This along with analysis of the solar radiation incident upon the external surface of the membrane allows the intensity of solar radiation directed in to the space by the internal surface of the membrane ($q_\tau$), and the total solar absorption of the membrane ($q\alpha$) to be determined.

$$q_\alpha = q_{\alpha(int)} + q_{\alpha(ext)}$$

$$q_\tau = q_{\tau(int)} + q_{\tau(ext)}$$

The total solar radiation directed into the space by the membrane panel is then output to the *Time Series Data Base of Environmental Conditions*, and the total solar radiation which it absorbs is used by the *Heat Transfer Model* in order to determine the internal surface temperature of the membrane, as described overleaf.

## 7:4    DESCRIPTION OF THE HEAT TRANSFER MODEL.

### 7:4.1    Introduction.

The monitored behaviour previously discussed in Chapter 5 had suggested that the fabric membrane samples investigated had insufficient thermal mass to significantly affect their thermal behaviour. At any instant therefore a single panel of a membrane may be assumed to be at its *equilibrium temperature* which represents the temperature at which there is no net heat transfer between the membrane panel and its surroundings. This means that if the equilibrium temperature of a membrane is tracked through time, this should give a good approximation of its transient behaviour.

The equilibrium temperature of a membrane can be determined by calculating that temperature at which the sum of all its individual heat transfers is equal to zero. These heat transfers consist of the long wave infra red radiation and convection heat transfers of both its surfaces, and the solar absorptance of its core material.

In order to properly simulate this situation, the *Heat Transfer Model* treats the membrane panels as consisting of two halves, each representative of one of the membranes surfaces, and each linked to the other by the conductivity of the membrane core.

*Figure 7:4.1 The Heat Transfer Model Representation of the Thermal Behaviour of Fabric Membranes.*
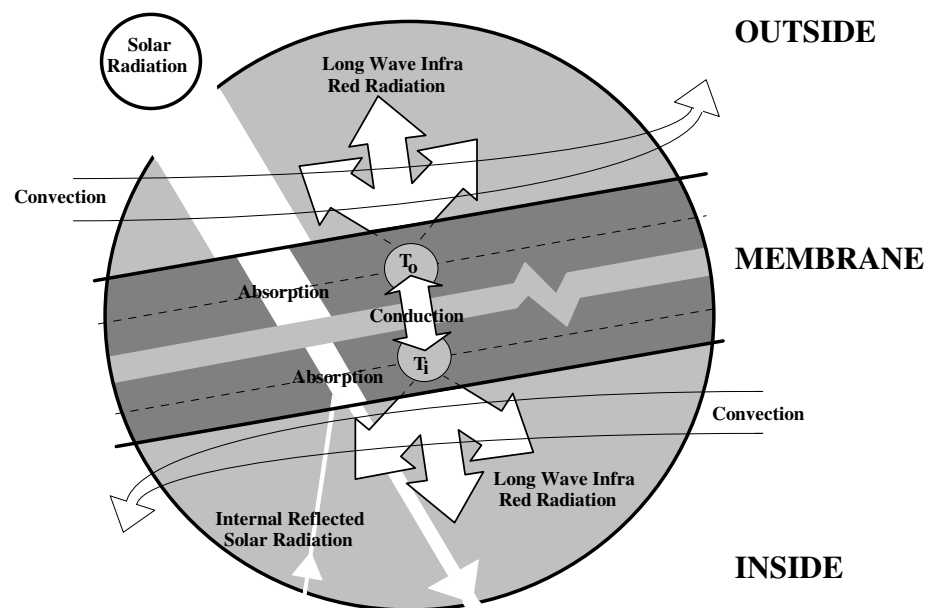
7:4.2    **The Convergence Procedure.**

The sequence of events carried out in order to determine the *equilibrium temperature* of the membrane, and the progression of the model through the time series of environmental conditions is regulated by the *Control Programme*.

The model converges on the equilibrium temperature of the membrane by a process of iteration. This is done by repeatedly '*guessing*' the temperature of the membrane and then calculating its net heat transfer with its surroundings at that temperature. If the calculated net exchange of heat is from the membrane to its surroundings, then the predicted membrane temperature is hotter than its equilibrium temperature. If the calculated net exchange of heat is into the membrane from its surroundings, then the predicted temperature is colder than its equilibrium temperature.

As the membrane is considered to be composed of two halves, two iterative processes are carried out. First the temperature of the external half of the membrane ($T_O$) is varied until its net heat transfer with its surroundings is zero, and then whilst $T_O$ remains fixed, the temperature of the internal half of the membrane ($T_i$) is varied until the its net heat transfer with its surroundings is zero. This procedure is repeated a number of times, and following successive iterations the sum of the two surface net heat transfers will tend towards zero, i.e. the model converges on the equilibrium temperature of the membrane.

Because this convergence procedure is an iterative one however, it is possible that an exact solution will never be reached. For this reason the model user is required to specify a termination residual such that when the net heat transfer of both halves of the membrane is below this value, it is considered to have converged on a solution. As a default, the termination residual is set at $0.0001\text{W/m}^2$ which should be very close to the exact solution.

Once a solution has been reached, the model output information is transferred to the *Time Series Data Base of Environmental Conditions* were it is recorded along side the input information. The *Control Programme* then checks to see whether there are any more time steps to run through. If there are, it removes the solved time series input information and the solution output data from the active line position of the *Time Series Data Base of Environmental Conditions*, and replaces this with the input information for the next time step. The whole process is then be repeated.

This procedure is illustrated schematically by *Figure 7:4.2* overleaf.

*Figure 7:4.2 Schematic Illustration of the Convergence Procedure.*
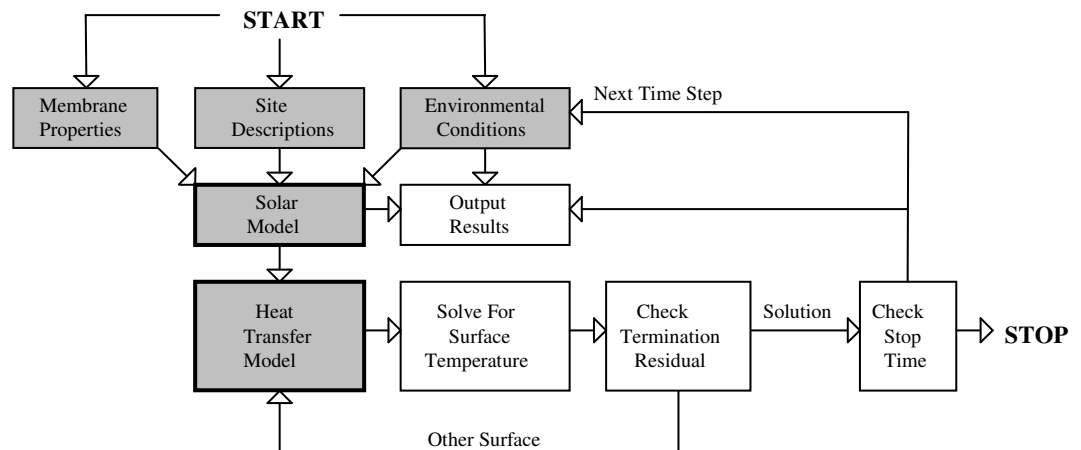


The next five parts of this section discuss in more detail the specific calculations carried out by the *Heat Transfer Model* in order to predict the net heat transfer of the membrane surfaces with their surroundings. These calculations are categorised as:-

- Calculation of the external surface long wave infra red radiation heat transfer.
- Calculation of the internal surface long wave infra red radiation heat transfer.
- Calculation of the external surface convection heat transfer.
- Calculation of the internal surface convection heat transfer.
- Calculation of the membrane core behaviour.

7:4.3 **Calculation of the External Surface Long Wave Infra Red Radiation Heat Transfer.**

The purpose of these calculations is to determine the long wave infra red radiation exchange between the external surface of the membrane panel and the hemisphere of surfaces facing it as a result of a temperature difference between them.

These calculations are based on estimating the average temperature of the hemisphere of surfaces facing the membrane. This is done by calculating the temperature of the individual surfaces making up that hemisphere, and the determining the relative views which the membrane panel has of these surfaces. To simplify this complex situation these surfaces are categorised as *ground*, *sky* and *obstruction* surfaces.

The proportion of the external hemisphere occupied by these surfaces are described as *view factors*, and these have previously been determined in order to calculate the reflected solar radiation incident upon the external surface of the membrane panel ( *Figure 7:3.3* ). This means that it is only necessary to estimate their average temperatures.

•     The method for determining the *sky temperature* is well established, but requires that the extent of cloud cover is known. This can be calculated during hours of daylight by comparing the intensity of monitored horizontal global solar radiation with that amount which could theoretically have been recorded if the sky were perfectly clear (see section 7:3.2). Simulations of night time behaviour however required an alternative approach.

It was observed that the solarimeters used to measure the intensity of horizontal global solar radiation during the day, emitted small amounts of radiation themselves during the night. The negative values recorded by the logging equipment as a result of this were roughly proportional to the *sky temperature* observed by the solarimeter.

The largest negative solarimeter reading recorded was -3.1mv, and so from this a scale was established from which night time cloud cover (N) is approximated.

$$N = ( \text{negative reading} + 3.1 ) / 3.1$$

Form the *external air temperature* ($t_o$), it is possible to estimate the long wave infra red radiation which would be incident on a horizontal surface under a clear sky ($H_{ac}$):-

$$H_{ac} = 1.06 \, \sigma \, ( t_o + 273.15)^4 - 11.9 \qquad [23]$$

From this, it is possible to determine the *apparent emittance* of the clear sky ($\varepsilon_{ac}$):-

$$\varepsilon_{ac} = H_{ac} / \sigma \, ( t_o + 273.15 )^4 \qquad [24]$$

The estimation of *cloud cover* and the *clear sky emittance* can then be used to predict the *cloudy sky horizontal apparent emittance* ($\varepsilon_{am}$):-

$$\varepsilon_{am} = ( 1 - 0.84 \, N ) \, \varepsilon_{ac} + 0.84 \, N \qquad [25]$$

and from this, the *cloudy sky long wave infra red radiation* incident upon a surface of inclination $\beta$ can be predicted:-

$$H_a = [\varepsilon_{am} \cos^2(\beta/2) + 0.03(1 - 0.84N) \, (\sin\beta)^{1.4}] \times \sigma \, (t_o + 273.15)^4 \qquad [26]$$

For the purposes of calculating hemispherical long wave infra red radiation exchange, this is more conveniently described as an *equivalent sky temperature*:-

$$T_{sky} = ( H_a / \sigma )^{0.25} \qquad [27]$$

- In order to accurately predict the temperature of the *ground* and other *obstructions* it would be necessary to go through the same process of dynamic calculation that the model already carries out in order to determine the surface temperature of the membrane panel itself. To include such a process within the model would be prohibitively complicated and so instead, the likely temperature of these surfaces is approximated based on the known thermal behaviour of a range of commonly occurring materials.

The combination of the types of surface surrounding the membrane have already been specified by the user from a list of commonly occurring materials (see Section 7:3.3), and the intensity of solar radiation incident upon them has been determined. The temperature of these materials can be estimated therefore from their known thermal behaviour, based on the external air temperature and the intensity of solar radiation incident upon their surface.

The model considers that the *maximum* intensity of solar radiation which could be incident upon these surfaces is about $1200W/m^2$. A scale is calculated based upon this and the intensity of solar radiation which is actually incident upon the surfaces, and this allows their temperature to be predicted relative to the external air temperature.

$$T = t_o - T_{min} + [ ( I / 1200) \times ( T_{max} - T_{min} )]$$

where I is the intensity of solar radiation incident upon the surface of the material, and $T_{max}$ and $T_{min}$ are the extreme temperatures that those materials had been observed to reach compared to the temperature of the air around them, as defined by the table below:-

*Figure 7:4.3 Table to Illustrate the Extreme Differences Between the External air Temperature and the Surface Temperatures of a Range of Commonly Occurring Materials.[28].*

| Material | Maximum surface temperature above air temperature (°c) $T_{Max}$ | Maximum surface temperature below air temperature (°c) $T_{Min}$ |
|---|---|---|
| new concrete | +5 | -1 |
| old concrete | +7 | -1 |
| grass | +5 | -2 |
| crushed rock | +17 | 0 |
| bitumen and gravel roof | +18 | 0 |
| bitumen road | +20 | 0 |

- Based upon the *sky* temperature and the temperature of the *ground* and other *obstructions*, the effective black body surface temperature of the external hemisphere ($T_e$) can be predicted:-

$$T_e = [ (V_{sky} \times T_{sky})^4 + (V_{grd} \times T_{grd})^4 + (V_{obs} \times T_{obs})^4 ]^{1/4} \qquad [29]$$

where $V_{sky}$, $V_{grd}$ and $V_{obs}$ are the sky, ground and obstruction view factors respectively, and $T_{sky}$, $T_{grd}$ and $T_{obs}$ are their temperatures. And hence the long wave infra red radiation surface exchange between the membrane panel and the hemisphere surrounding its external surface can be calculated:-

$$q_{lwo} = \varepsilon_o \times \sigma [ (T_e)^4 - (T_o)^4 ] \qquad [30]$$

where $\varepsilon_o$ is the emissivity of the external surface of the membrane panel, and $\sigma$ is the Steffan- Boltzmann constant ($5.6697 \times 10^{-8} W/m^2 {}^o k^4$).

### 7:4.4    Calculation of the Internal Surface Long Wave Infra Red Radiation Heat Transfer.

These calculations were carried out in order to determine the long wave infra red radiation exchange between the internal surface of the membrane panel and the hemisphere of surfaces facing it as a result of a temperature difference between them.

The geometry of the enclosed space is not specified within the model, and so it is necessary to make some assumptions about the internal surfaces with which the membrane is in radiant communication.

The average temperature of internal surfaces facing the membrane is specified by the user ($t_{is}$). Because of the geometry of such spaces however the membrane panel can be facing both this representative internal surface, and other parts of the membrane enclosure itself. As the inclination of the membrane panel ($\beta$) is known, a fairly good guess can be made of the relative view that the membrane has of these two elements and so an *equivalent internal surface temperature* ($t_q$) can be calculated.

$$t_q = \{[ (\beta / 180) T_i^4 ] + \{[ 1- (\beta / 180) ] t_{is}^4 \}\}^{1/4}$$

It is recognised that $T_i$ may not be representative of the behaviour of the entire membrane boundary, but as the membrane can display extreme thermal behaviour it is considered that this is more appropriate than assuming that the panel faced only the thermally stable '*conventional*' surfaces of the interior.

In the case of the test cell however, where there is only one membrane panel to consider, the monitored internal surface temperature of the test cell is considered entirely representative of the thermal state of the internal hemisphere.

A similar process is then carried out in order to estimate an *equivalent emissivity* representative of the surfaces with which the membrane panel was communicating ($\varepsilon_{eq}$).

$$\varepsilon_{eq} = [ \, \varepsilon_i \, ( \, \beta \, / \, 180 \, )] + \{ \, \varepsilon_{int} \, [ \, 1 - ( \, \beta \, / \, 180 \, ) \, ] \, \}$$

And from this an *emissivity factor* ($F_\varepsilon$) *i*s calculated describing the net emissivity between the membrane and the internal hemisphere:-

$$F_\varepsilon = \cfrac{1}{\cfrac{1}{\varepsilon_i} + \cfrac{1}{\varepsilon_{eq}} - 1} \qquad\qquad [31]$$

The net long wave infra red radiation exchange between the internal surface of the membrane panel and the enclosed space can then be calculated:-

$$q_{lwi} = F_\varepsilon \times \sigma \, [ \, ( \, t_q \, )^4 - (T_i \, )^4 \, ] \qquad\qquad [32]$$

### 7:4.5 Calculation of the External Surface Convection Heat Transfer.

These calculation are carried out in order to predict the net heat transfer between the external surface of the membrane and the external air close to it, as a result of a temperature difference between them. The procedure adopted for this purpose is well established, if a little simplistic.

The azimuth of the membrane surface is categorised as facing either *windward* or *leeward*. A *surface wind velocity* (V) is then calculated based on the measured *free stream wind speed* ($V_f$) relative to this surface orientation.

windward          if      $V_f > 2m/s$      $V = 0.25 \, V_f$

                       if      $V_f < 2m/s$      $V = 0.5$

leeward                    $V = 0.3 + 0.05 \, V_f$      [33]

An expression developed by McAdams can then used to determine an external surface convection heat transfer coefficient[34]:-

$$h_{co} = 5.678 \left[ a + b \left( V / 0.3048 \right)^n \right]$$

where          if V < 4.88m/s,          a = 0.99          b = 0.21          n = 1
               if 4.88 ≤ V < 30.48          a = 1.09          b = 0.23          n = 1

And from this, the external surface convection heat transfer can then be calculated:-

$$q_{cvo} = h_{co} \times A \left( t_o - T_o \right)$$

## 7:4.6    Calculation of the Internal Surface Convection Heat Transfer.

These calculations are carried out in order to determine the quantity of heat transferred between the internal surface of the membrane and the air close to it as a result of a temperature difference between them. As with external surface convection, this is done by calculating a surface convection heat transfer coefficient and then using this to predict the net convection heat transfer. For this purpose, three basic types of *internal surface convection heat transfer coefficient* ($h_{ci}$) can be calculated relating to common natural convection conditions:-

- Heat transfer between the enclosed air and a vertical surface:-

$$h_{ci} = \left\{ \left[ 1.5 \left( \frac{|t_i - T_i|}{L} \right)^{\frac{1}{4}} \right]^6 + \left( 1.23 \times |t_i - T_i|^{\frac{1}{3}} \right)^6 \right\}^{\frac{1}{6}}$$          [35]

- Heat transfer between the enclosed air, and a horizontal surface where buoyancy forces will tend to draw the affected air away from the surface, i.e. air warming up above a horizontal surface or cooling down below a horizontal surface:-

$$h_{ci} = \left\{ \left[ 1.4 \left( \frac{|t_i - T_i|}{L} \right)^{\frac{1}{4}} \right]^6 + \left( 1.63 \times |t_i - T_i|^{\frac{1}{3}} \right)^6 \right\}^{\frac{1}{6}}$$          [36]

- Heat transfer between the enclosed air, and a horizontal surface where buoyancy will tend to push the affected air back into the surface, i.e. air warming up *below* a horizontal surface or cooling down *above* a horizontal surface.

$$h_{ci} = 0.6 \; ( \; |t_i - T_i| \; / \; L^2 \; )^{0.2} \hspace{3cm} [37]$$

where $T_i$ represents the internal surface temperature of the membrane, $t_i$ the temperature of the air film close to the surface, and L the *characteristic length* of the surface.

These relationships were originally developed from investigations into the movement of air through ducts and pipes where the term *characteristic length*, described the diameter of the duct. Its re application to the built environment however has required that new interpretations of *characteristic length* be developed[38].

Horizontal surface             L = 4 × Surface area / Surface perimeter length

Vertical surface              L = Surface height

The validity of applying these equations to spaces enclosed by doubly curved fabric membranes however, where concepts such as *surface height* have little meaning, is a little difficult to judge.

The three categories of internal surface natural convection heat transfer described above were developed primarily for investigating the thermal behaviour of conventional building surfaces which tend to be either vertical or horizontal. Doubly curved membrane surfaces however are more difficult to categorise.

Research by Fishendem has suggested that it is not inappropriate to extrapolate between vertical and horizontal values of $h_{ci}$ in order to represent inclined surfaces[39], and the model therefore adopts a linear weighting to account for surface inclination (β):-

$$h_{ci \; (\beta)} = \{[\beta \times h_{ci \; (vertical)}] + [ \; ( \; 90 - \beta \; ) \times h_{ci \; (horizontal)}]\} \; / \; 90$$

The model also provides a forced convection option for those spaces in which artificial ventilation is likely to disturb the enclosed air, resulting in an increase in internal surface convection heat transfers.

$$h_{ci} = 5.678 \; [ \; 0.99 + 0.21 \; ( \; V_p \; / \; 0.3048) \; ] \hspace{3cm} [40]$$

where $V_p$ is a parallel flow velocity representative of air movement within the space.

The internal surface convection heat transfer can then be calculated by selecting one of the approaches described above and inserting the appropriate heat transfer coefficient into the standard equation below:-

$$q_{cvi} = h_{ci} \times A\ (\ t_i - T_i\ ) \qquad\qquad [41]$$

### 7:4.7 Calculation of the Membrane Core Behaviour.

These calculations are carried out in order to quantify the total net power exchange of the two halves of the membrane panel with their surroundings.

- The surface *convection* and *long wave infra red radiation* exchanges are treated simply as net transfers between the relevant half of the membrane and its surrounding hemisphere.

- The *conductance* between the two halves of the membrane is calculated as the product of half the conductivity of the its core material and the difference in the temperature of its two halves.

$$q_{condi} = (C_{core} / 2) \times (T_o - T_i) \qquad\qquad q_{condo} = (C_{core} / 2) \times (T_i - T_o)$$

where $q_{condi}$ represents the net conduction heat transfer of the internal half of the membrane, and $q_{condo}$ represents the net conduction heat transfer of the external half of the membrane.

- Separating *solar absorption* between the two halves of the membrane panel however is considerably more complex. Solar radiation is progressively absorbed by the membrane panel as it passes through it and so in order to calculate how much is absorbed by each half of the membrane it is be necessary to determine the rate of absorption per unit depth of the membrane.

This is done by calculating the *extinction coefficient* (K) which describes the progressive absorption of a known wavelength of radiation as it passes through a material with known optical properties. When K is known, the remaining solar radiation ($I_d$) at depth $\delta$ into a material can be calculated:-

$$I_d = I\ (\ \alpha + \tau\ )\ e^{-K\delta} \qquad\qquad [42]$$

where I is the intensity of incident radiation, $\alpha$ is the absorptance of the material, and $\tau$ is its transmittance.

For fabric membranes two extinction coefficients were calculated ($K_{int}$ and $K_{ext}$) one for the external incident solar radiation ($I_d + I_f$) and one for the internal incident solar radiation ( $q_{\rho(int)} + q_{\tau(int)} + q_{\alpha(int)}$ ):-

$$K_{ext} = \frac{-\ln\left(\frac{q_{\alpha(ext)} + q_{\tau(ext)}}{q_{\tau(ext)}}\right)}{g} \qquad\qquad K_{int} = \frac{-\ln\left(\frac{q_{\alpha(int)} + q_{\tau(int)}}{q_{\tau(int)}}\right)}{g} \qquad [43]$$

So that at depth $\delta$ into the membrane the remaining intensity of internal incident and external incident solar radiation ( $I_{\delta(int)}$ and $I_{\delta(ext)}$ ) can be calculated:-

$$I_{\delta(int)} = \left[q_{\rho(int)} + q_{\tau(int)} + q_{\alpha(int)}\right] \times \left(\tau_{(f)} + \alpha_{(f)}\right) e^{\left[-K_{(int)} \times (g-\delta)\right]}$$

$$I_{\delta(ext)} = \left(I_d + I_f\right) \times \left[\frac{q_{\alpha(ext)}}{I_d + I_f} + \frac{q_{\tau(ext)}}{I_d + I_f}\right] e^{\left[-K_{(ext)} \times \delta\right]}$$

The total solar absorption of each half of the membrane ( $\alpha_{(ext)}$ and $\alpha_{(int)}$ ) can then be calculated from the sum of these two absorption processes where $\delta$ is taken to equal g/2.

$\alpha_{(ext)} = I_{\delta(int)} + I_{\delta(ext)}$

$\alpha_{(int)} = q_{\tau(int)} + q_{\alpha(int)} + q_{\tau(ext)} + q_{\alpha(ext)} - \alpha_{(ext)}$

From this it is possible to calculate the total net heat transfer of the two membrane halves:-

net internal surface heat transfer $\qquad\qquad q_i = q_{cvi} + q_{lwi} + q_{\alpha(int)} + q_{condi}$

net external surface heat transfer $\qquad\qquad q_o = q_{cvo} + q_{lwo} + q_{\alpha(ext)} + q_{condo}$

and so the total net membrane heat transfer q can be calculated:-

$q = q_i + q_o$

When $T_o$ and $T_i$ are such that q is less than $0.0001 W/m^2$, it is considered that the membrane is at its *equilibrium temperature.*

## 7:5.  COMPARISON BETWEEN THE MODEL OUTPUT AND MONITORED DATA.

### 7:5.1  Introduction.

In this section an investigation into the accuracy of the membrane boundary model is described. For this purpose the same model categorisation is adopted as was used in the previous two sections of this chapter:-

- The *Solar Model*, developed in order to predict the intensity of solar radiation directed into the enclosure by the membrane panel.
- The *Heat Transfer Model,* developed in order to predict the internal surface temperature of the membrane panel.

The accuracy of these two models was tested against the behavioural data obtained from the test cell and associated meteorological station, previously presented and discussed in Chapter 5.

### 7:5.2  Comparison Between the Output of the Solar Model and Monitored Data.

It had not been possible to use the test cell described in Chapter 5 to obtain data regarding the intensity of solar radiation within the test cell. This meant that the accuracy of the solar model had to be determined from the sum of two parts for which data was available:-

- The intensity of solar radiation incident upon the external surface of the membrane had been recorded using the test cell, and so the ability of the model to accurately predict this could be tested.
- The accuracy of the equations used to predict the angular solar optical properties of the membranes described in Chapter 6 was already known.

This meant that if the net error resulting from these two processes could be calculated, then this could be considered to represent the overall ability of the model to predict the intensity of solar radiation transmitted through a membrane panel of known orientation.

The graphs overleaf relate to the first part of this calculation, illustrating the relationship between the monitored solar radiation incident on the external surface of the membrane samples, and that predicted by the solar model. As these predictions were based upon the measured horizontal global soar radiation, there was obviously no error at all for the horizontal panels monitored. Because of this, only data from the three test cell investigations carried out using inclined membrane panels is illustrated.

*Figure 7:5.2a Solar Model Simulation: 16/9/94. Inclination 59⁰, Azimuth 47.5⁰ East of South.*
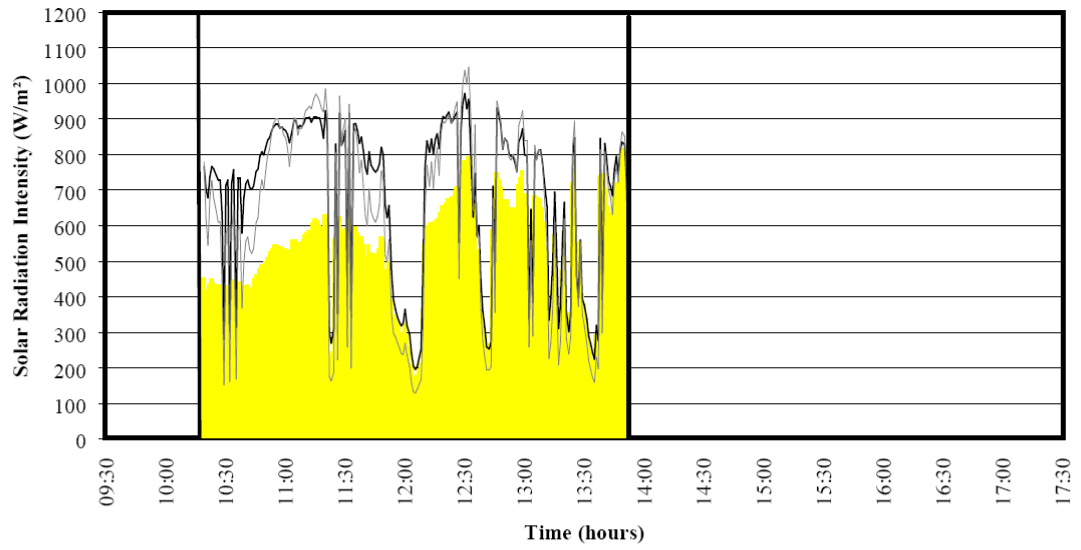


*Figure 7:5.2b Solar Model Simulation: 20/0/94. Inclination 60.5⁰, Azimuth 46.3⁰ East of South.*
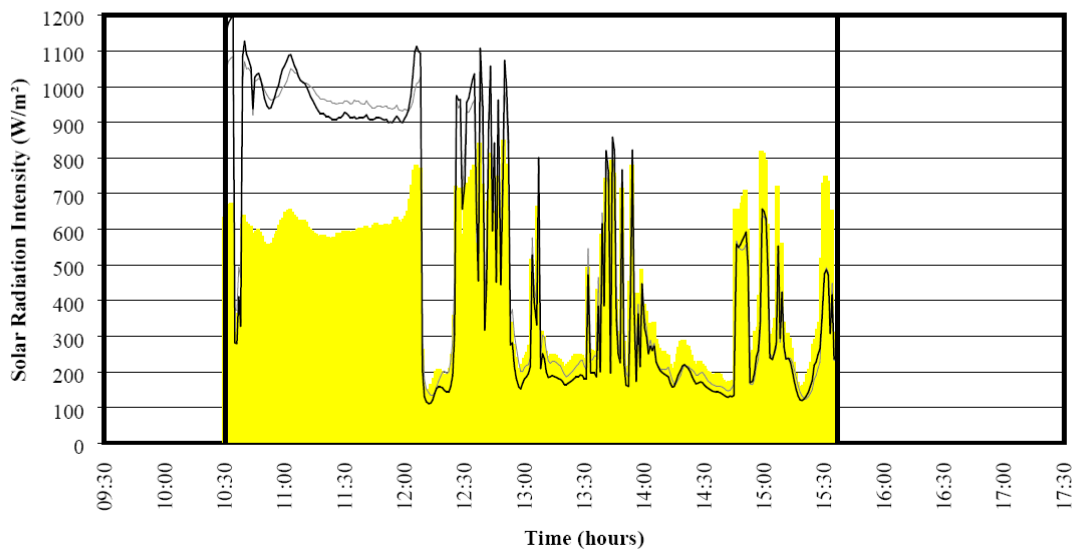


| | | |
|---|---|---|
| Horizontal Global Solar Radiation | Monitored Incident Solar Radiation | Predicted Incident Solar Radiation |

*Figure 7:5.2c Solar Model Simulation: 10/10/94. Inclination 67°, Azimuth 41° East of South.*
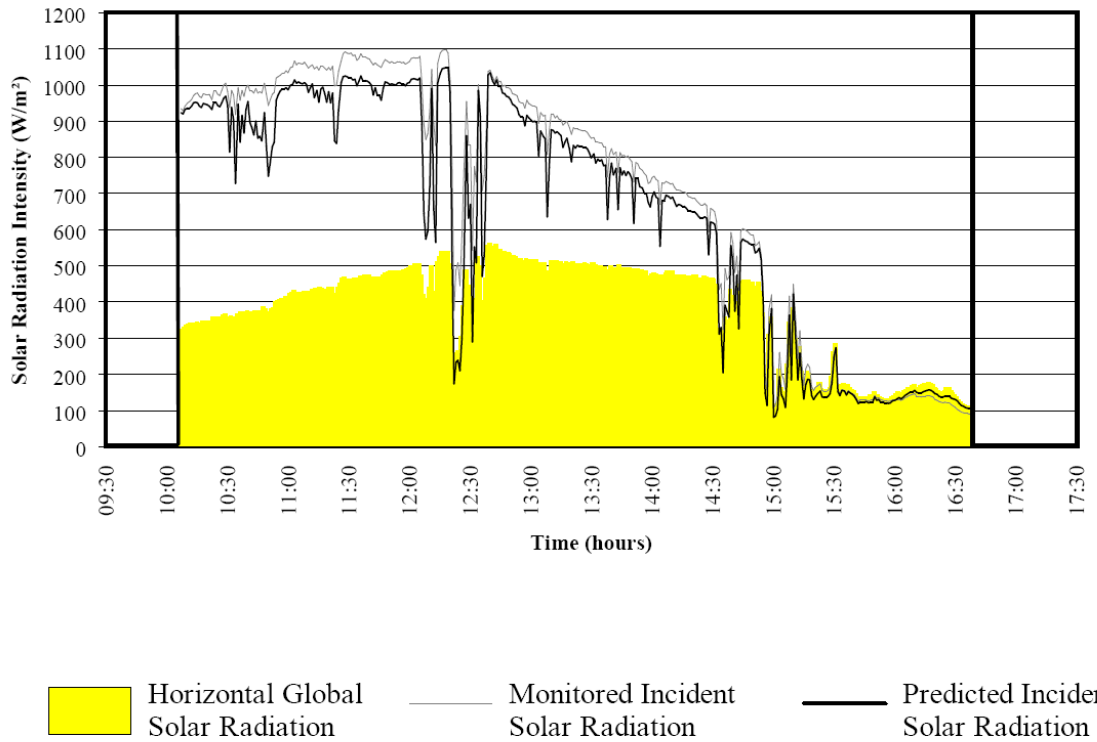


The average difference between the predicted and monitored incident solar radiation illustrated by the above graphs was just $50W/m^2$ or 10%, however the maximum error was almost $235W/m^2$. The graph below illustrates how the trend of these errors varied with the intensity of solar radiation. The ideal relationship is represented by the diagonal line.

*Figure 7:5.2d Diagram to Show the Relationship Between Predicted and Monitored Solar Radiation Incident upon Surfaces of Inclination from 55 to 70°.*
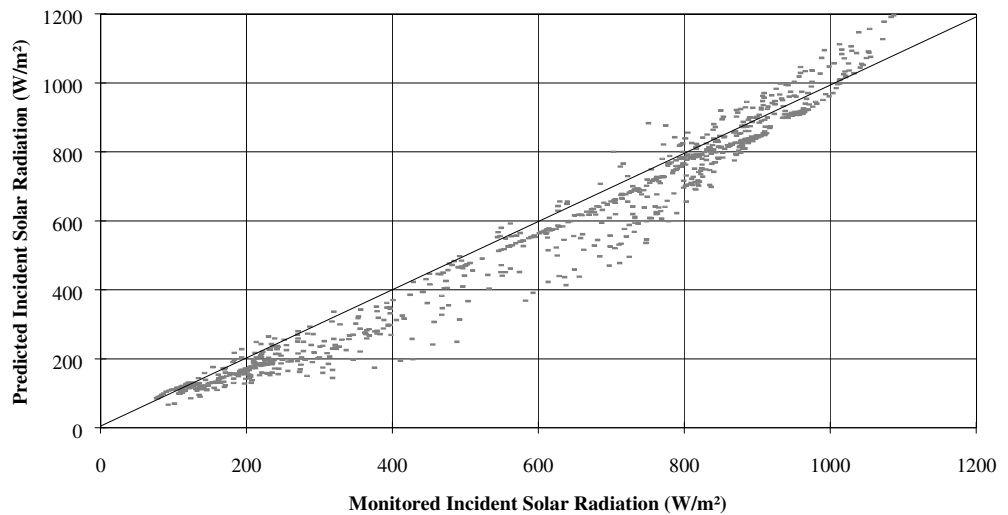
It can be seen that the model tended to under predict the intensity of solar radiation during overcast conditions, but to over predict it during bright sunshine. Comparison of the solar model output with the data available from the test cell meteorological station revealed that this resulted from a propensity to underestimate horizontal diffuse solar radiation by an average of 11%. This in turn appeared to result from the under prediction of *theoretical clear sky solar radiation* which led to an underestimation of *cloud cover*.

It is difficult to pinpoint the source of these errors, but the statistical estimates of turbidity and precipitable water content meant that such inaccuracies had always been likely. Whilst impractical for the short term site monitoring described in Chapter 8, it is recommended that in the future many uncertainties would be removed from these calculations if both horizontal *global* and horizontal *diffuse* solar radiation were monitored.

The compound error resulting from the solar predictions discussed above and the standard equations used to approximate angular solar optical properties described in Chapter 6 was then assessed. This was done by calculating the net error resulting from both processes when compared to the measured values for all six of data sets presented in Chapter 5.

***Figure 7:5.2e Table to Summarise the Predicted Errors Associated with the Solar Model.***

|  | Solar Radiation Reflected by the Membrane Samples (W/m$^2$) | Solar Radiation Absorbed by the Membrane Samples (W/m$^2$) | Solar Radiation Transmitted by the Membrane Samples (W/m$^2$) |
|---|---|---|---|
| Average Error | 16.5 | 4.3 | 3.5 |
| Maximum Error | 175.5 | 31.2 | 17.4 |

This level of precision was considered sufficient to allow the accurate simulation of the thermal behaviour of fabric membranes and the spaces enclosed by them.

### 7:5.3 Comparison Between the Output of the Heat Transfer Model and Monitored Data.

The fundamental purpose of the *Heat Transfer Model* was to predict the equilibrium internal surface temperature of the membrane panel being investigated. The 6 test cell investigations previously described in Chapter 5 provided a comprehensive range of behavioural data with which to test the accuracy of these predictions.

The graphs overleaf illustrate the monitored and predicted membrane internal surface temperatures for the entire data set. These graphs are the same as those presented in Chapter 5, but with the *predicted* membrane internal surface temperatures superimposed.

*Figure 7:5.3a Thermal Simulation: Type 1 PVC Coated Polyester.*
**16/9/94**, Inclination **59.2⁰**, Azimuth **47.6⁰** East of South.
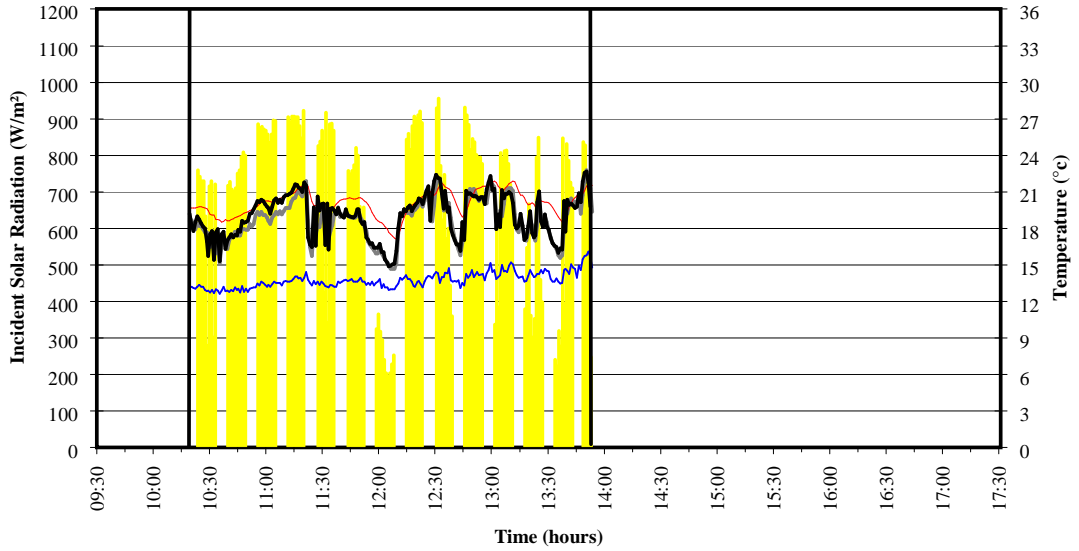


*Figure 7:5.3b Thermal Simulation: PTFE Coated Glass (New).*
**20/9/94**, Inclination **60.5⁰**, Azimuth **46.3⁰** East of South.

Incident Solar Radiation

External Air Temperature — Predicted Membrane Temperature

Internal Air Temperature — Monitored Membrane Temperature
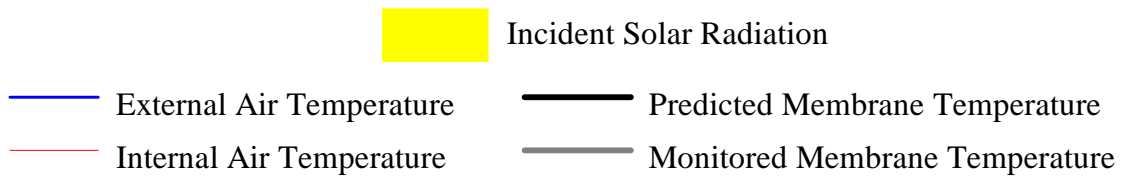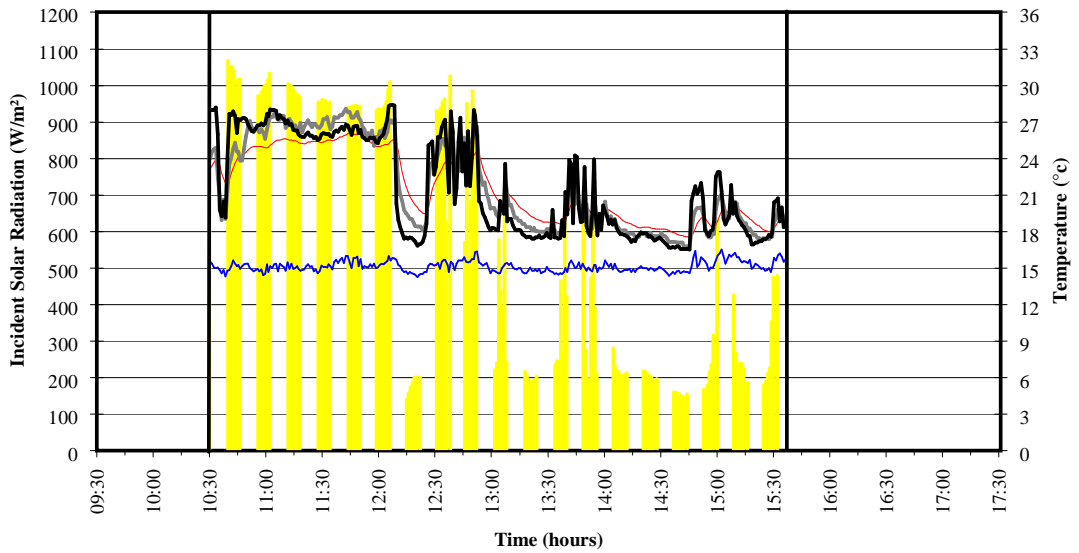
**Figure 7:5.3c Thermal Simulation: Type 2 PVC Coated Polyester.**
**10/10/94**, Inclination **66.9⁰**, Azimuth **40.8⁰** East of South.
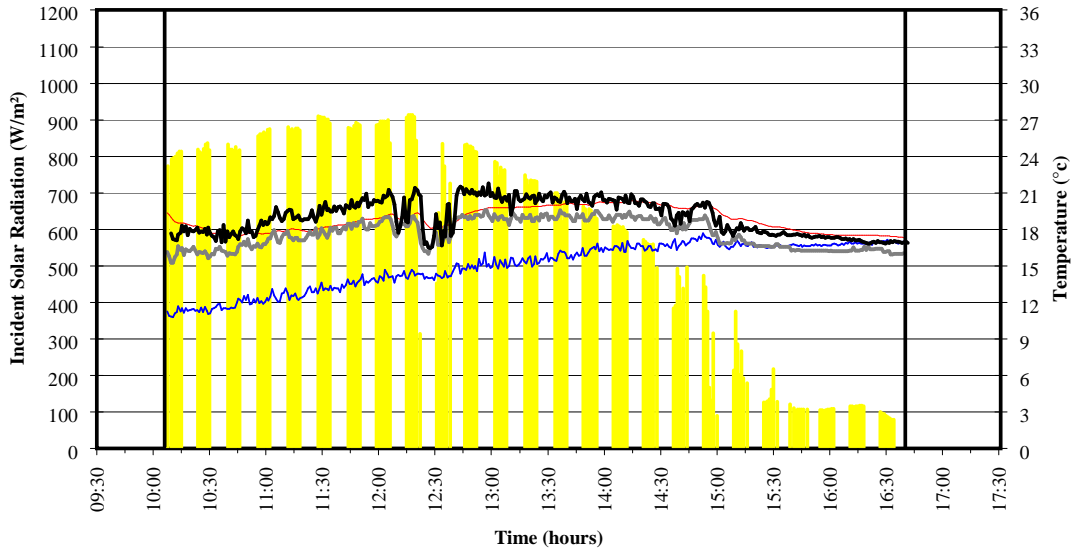


**Figure 7:5.3d Thermal Simulation: Type 3 PVC Coated Polyester.**
**16/12/94**, Inclination **0⁰**, Azimuth **n/a**.



Incident Solar Radiation

External Air Temperature — Predicted Membrane Temperature

Internal Air Temperature — Monitored Membrane Temperature
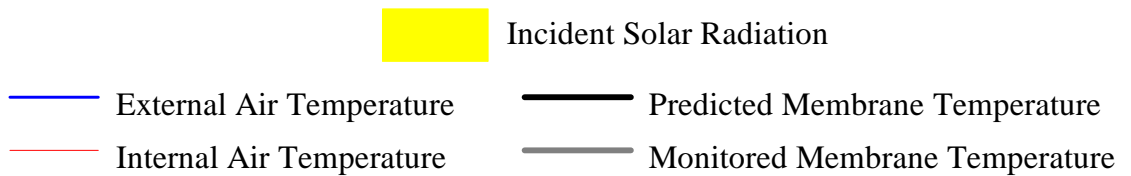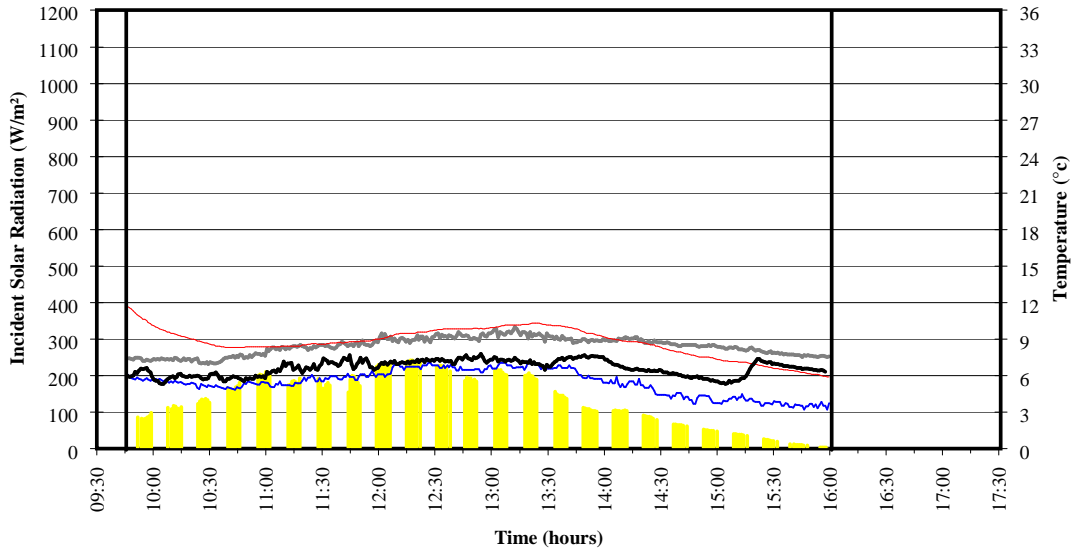
**Figure 7:5.3e Thermal Simulation: Eisteddfod Arena Membrane.**
**10/4/95**, Inclination **0⁰**, Azimuth **n/a**.
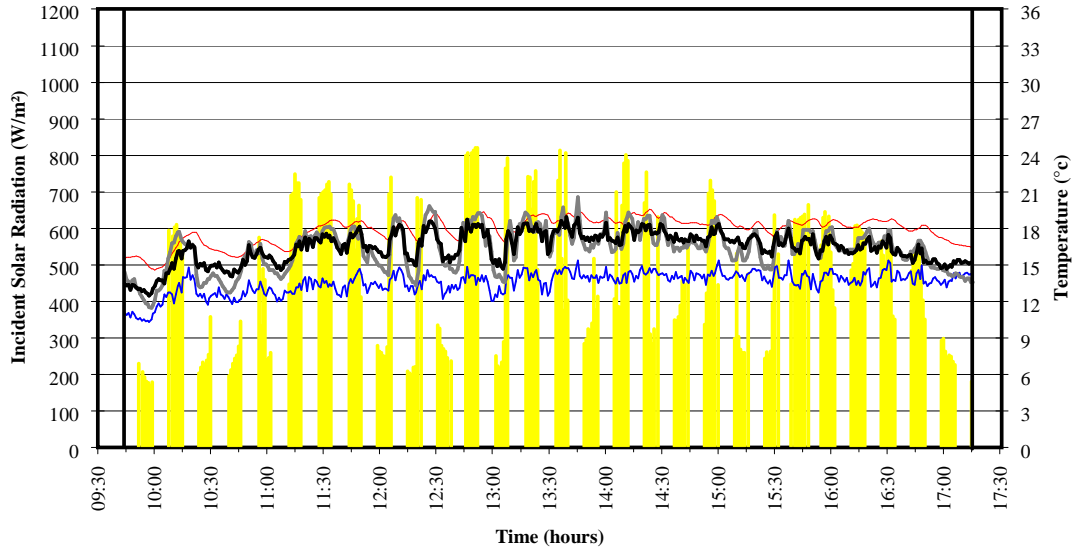


**Figure 7:5.3f Thermal Simulation: Type 4 PVC Coated Polyester.**
**3/5/95**, Inclination **0⁰**, Azimuth **n/a**.



Incident Solar Radiation

External Air Temperature — Predicted Membrane Temperature
Internal Air Temperature — Monitored Membrane Temperature
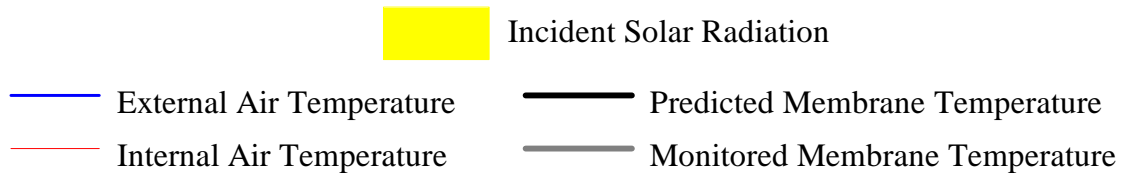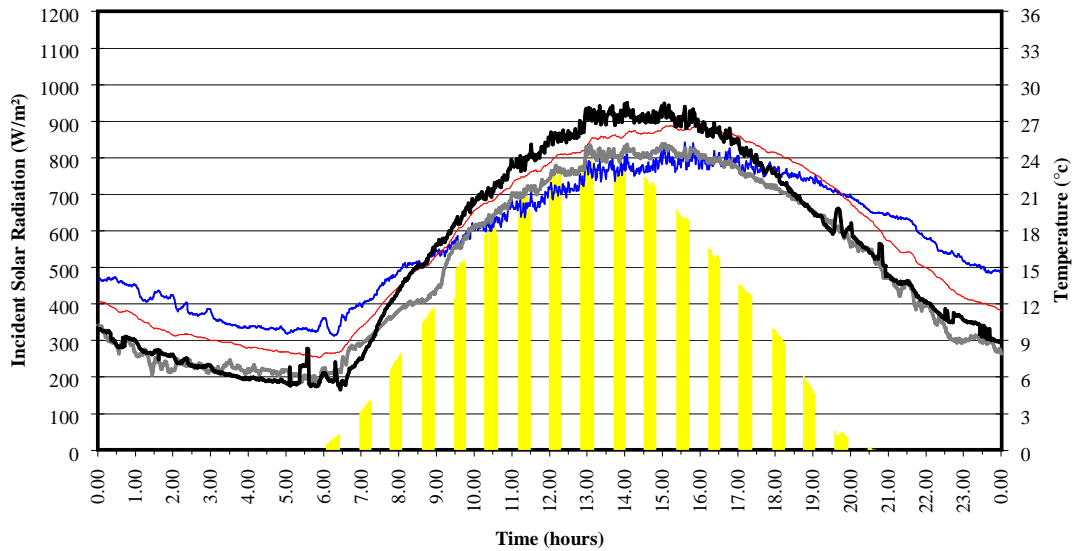
***Figure 7:5.3g Table to Summarise the Differences Between Predicted and Recorded Membrane Internal Surface Temperatures.***

| Membrane | Time Steps (mins) | Max +ve Error ($^{o}$c) | Max -ve Error ($^{o}$c) | Average Error ($^{o}$c) | Average Absolute Error ($^{o}$c) |
|---|---|---|---|---|---|
| Type 1 PVC coated polyester | 214 | +2.36 | -1.73 | +0.32 | \|0.59\| |
| Type 2 PVC coated polyester | 393 | +3.09 | -0.12 | +1.37 | \|1.37\| |
| Type 3 PVC coated polyester | 373 | +3.66 | -0.37 | +1.19 | \|1.20\| |
| Type 4 PVC coated polyester | 1442 | +3.92 | -2.10 | +1.17 | \|1.47\| |
| Eisteddfod Arena membrane | 454 | +2.18 | -2.24 | -0.12 | \|0.69\| |
| PTFE coated glass (new) | 307 | +4.20 | -4.12 | -0.12 | \|1.04\| |
| Overall | 3183 | +4.20 | -4.12 | +0.83 | \|1.21\| |

It can be seen from the above table that whilst the maximum model error was 4.2$^{o}$c, on average the predicted values were within 1.2$^{o}$c of the monitored data.

The graph below shows the actual relationship between the predicted and monitored internal surface temperatures. The ideal relationship is shown by the diagonal black line.

***Figure 7:5.3h The Relationship Between the Monitored Internal Surface Temperature and the Temperature Predicted Using The Dynamic Boundary Model.***
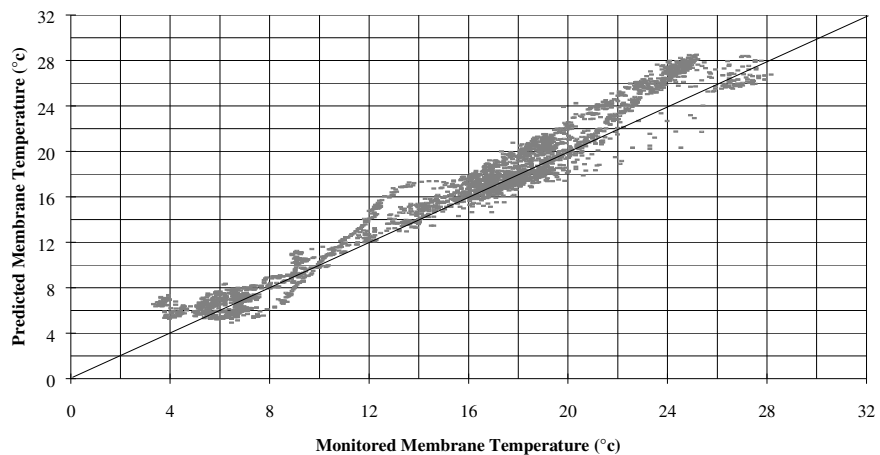


It can be seen that although errors were distributed fairly evenly on either side of the ideal, at higher temperatures there was a tendency for the model to increasingly overestimate the membrane temperature. These larger errors generally occurred during bright sunshine and this suggested that they may result directly from the tendency of the solar model to over predict the intensity of incident solar radiation under such conditions.

As was found in Chapter 5 however, beyond this simple level of analysis, the reasons for the model errors were difficult to assess without first breaking the results down into their component heat transfer calculations.

### 7:5.4 Analysis of the Heat Transfer Model Output.

An attempt was made to determine the sensitivity of the model predictions to the various heat transfer mechanisms affecting them. For this purpose, the model output was extended beyond those parameters required in order to describe the thermal state of the membrane itself, to include the six basic membrane heat transfers which it was considered could have some influence on the thermal behaviour of spaces enclosed by fabric membranes:-

- Membrane solar transmission.
- Membrane solar absorption.
- Membrane external surface long wave infra red radiation.
- Membrane internal surface long wave infra red radiation.
- Membrane external surface convection.
- Membrane internal surface convection.

These values were recorded for each time step investigated, and this had two basic aims:-

- *The identification of systematic inaccuracies within the model.*
- To establish *the relative significance of individual membrane heat transfer mechanisms*.

NB     Core conduction was not included here as this was a purely internal heat transfer, and the maximum difference between the predicted internal and external membrane surface temperatures for any of the data sets investigated was just $0.11^{o}$c. This seemed to confirm that the membrane samples investigated had insufficient thermal resistance to significantly affect their overall behaviour, and validated the assumption that the external surface temperature sensors described in Chapter 5 were unreliable.

- *The Identification of Systematic Inaccuracies.*
  The model proved to be more sensitive to the inaccuracies of thermal modelling than may have been expected from more conventional materials, and it was considered that this resulted from their low mass. Because their behaviour was produced by an instantaneous response to the heat transfers affecting them, their predicted behaviour was affected instantly by any inaccuracies in the calculation procedure. Such inaccuracies may be less evident from models developed in order to simulate more massive conventional materials as their thermal storage would result in errors being evened out over time.

An attempt was made to identify any direct relationships between the various predicted membrane heat transfers and the accuracy of the predicted membrane internal surface temperature, and this was intended to identify any systematic inaccuracies within the boundary code. It proved impossible however to clearly identify any such relationships. Whilst this suggested that there were no major mistakes within the model, it was also considered that this resulted from the entirely dynamic thermal behaviour of the fabric membranes investigated.

Each individual heat transfer calculation affected the temperature of the membrane, and the temperature of the membrane in turn affected each of the heat transfer calculations. The complex behaviour of the membrane samples at any instant is dependent upon a large number of interrelated parameters which are difficult to isolate. As a consequence of this, the accuracy of the boundary model was also dependent upon a large number of interrelated parameters which were similarly difficult to isolate.

- *The Relative Significance of Individual Membrane Heat Transfer Mechanisms.*
  The relative significance of the various membrane heat transfer mechanisms predicted by the boundary model across the full range of data investigated is summarised by *Figures 7:5.4a* and *7:5.4b* below. Other than *solar transmission* these values refer to heat transfer between the membrane and its surroundings such that membrane heat gains are positive and membrane heat losses are negative.

**Figure 7:5.4a Table to Summarise the Significance of the Various Modes of Heat Transfers Calculated by The Thermal Boundary Model.**

| | Max Heat Gain (W/m$^2$) | Max Heat Loss (W/m$^2$) | Average Heat Transfer (W/m$^2$) | Average Absolute Heat Transfer (W/m$^2$) |
|---|---|---|---|---|
| Solar Transmission. | 169 | 0 | 25 | 25 |
| Solar Absorption. | +243 | 0 | +61 | 61 |
| Ext Surface Long Wave IR Radiation. | 0 | -107 | -56 | 56 |
| Int Surface Long Wave IR Radiation. | +26 | -33 | +3 | 8 |
| Ext Surface Convection. | +34 | -101 | -10 | 26 |
| Int Surface Convection. | +7 | -5 | +1 | 1 |

*Figure 7:5.4b Graph to Illustrate the Significance of the Various Modes of Heat Transfers Calculated by The Thermal Boundary Model.*
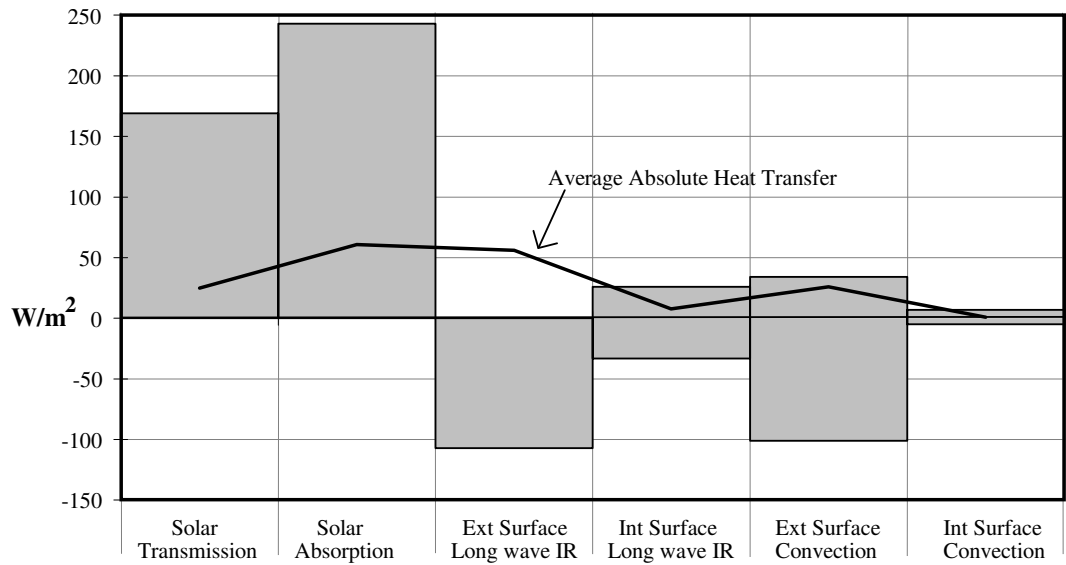


It can be seen from the above graph that solar radiation had the most significant affect on the total heat transfer across the membranes studied, both in terms of the net heat exchange between the membranes and their surroundings, and the quantity of solar radiation they transmitted directly into the spaces they enclosed. It is a little difficult to assess the exact significance of solar absorption and transmission in relation to other heat transfer mechanisms however as there was obviously no solar radiation during the nights.

Whilst solar absorption was generally higher than solar transmission, it can be seen that the majority of the solar radiation absorbed by the membrane was transferred back to the *outside* by radiation and convection, and not the *inside*. This suggested that solar transmission was the mechanism likely to most significantly affect the thermal behaviour of spaces enclosed by such membranes.

The maximum heat transfer by external surface long wave infra red radiation was just 107W/m$^2$ whilst the maximum solar absorption was 243W/m$^2$. However external surface long wave infra red radiation heat transfer occurred throughout the day, and this meant that its average value was almost as significant as solar absorptance.

The least significant external surface heat transfer mechanism was convection, although the amount of heat exchanged by this mechanism was actually surprisingly large considering the generally low wind speeds under which the test cell was monitored. The potential significance of this mechanism is illustrated by the fact that the maximum predicted external surface convection heat transfer was just 6W/m$^2$ less than the maximum predicted external surface long wave infra red radiation heat transfer.

Both internal surface convection and long wave infra red radiation heat transfers were comparatively insignificant. However it was considered that both this, and internal surface long wave infra red radiation heat transfers may have a more significant influence on the thermal behaviour of actual membrane roofed buildings than was suggested by the data collected from the test cell. This was because the difference between the temperature of the membrane and that of the full size enclosure was likely to be greater than was found with the low thermal mass test cell. This was likely to result in higher membrane internal surface heat transfers.

## 7:6.    CONCLUSION.

In this chapter a theoretical model was described which was developed in order to predict the thermal behaviour of fabric membranes. This model was specified using the properties data described in the Chapter 6, and its accuracy was tested against the behavioural data presented in Chapter 5. The compound errors produced by simulating these two sets of data are summarised by the table below.

*Figure 7:6. Table to Summarise the Overall Errors Associated with the Boundary Model.*

|  | Solar Radiation Reflected by Membrane Samples (W/m$^2$) | Solar Radiation Absorbed by Membrane Samples (W/m$^2$) | Solar Radiation Transmitted by Membrane Samples (W/m$^2$) | **Membrane Internal Surface Temp ($^o$c)** |
|---|---|---|---|---|
| Average Error | 16.5 | 4.3 | 3.5 | **1.2** |
| Maximum Error | 175.5 | 31.2 | 17.4 | **4.2** |

There was no evidence to contradict the fundamental assumption that thin fabric membranes have insufficient thermal mass to significantly affect their thermal behaviour. Because of this however, it was apparent that every modelling inaccuracy and oversimplification was instantly exposed in the predicted membrane behaviour.

This low mass, also meant that the thermal behaviour of the fabric membranes investigated was almost entirely dependent upon their surface heat transfers and solar absorptance. Whilst solar absorption and external surface long wave infra red heat transfer appeared to have the greatest influence on this behaviour, other perhaps less well researched mechanisms such as external surface convection were also of considerable significance. The great number of simplifications associated with these surface heat transfer calculations meant that significant modelling inaccuracies were inevitable.

Despite these limitations however, the average difference between the predicted and monitored internal surface temperatures of the membranes investigated was just $1.2^\circ$c. Similarly, the average difference between the predicted and monitored intensity of solar radiation directed in to the enclosed space by the membrane was less than 4W/m$^2$.

This suggested that the model was sufficiently accurate to provide the boundary information necessary to allow the thermal behaviour of spaces enclosed by such membranes to be investigated. Such an investigation is described in the next two chapters of this thesis.

NB    No heat transfer calculations were included to account for evaporation. The test cell construction was such that it could only be used on dry days, and rainfall was not recorded during the programme of spatial monitoring described in Chapter 8. Future investigations however should recognise the significance of this mechanism, particularly in hot climates.

[1]    Clarke, J. A; *Energy Simulation in Building Design*, Adam Hilger Ltd, Bristol, 1985, P323.

[2]    Page, Prof. J; Lebens, R (editors), *Climate in the UK: A handbook of solar radiation, temperature and other data for 13 principal cities and towns*, HMSO, London, 1986, P329.

[3]    ibid. Page, Prof. J et al, *Climate in the UK...,* P329.

[4]    ibid. Clarke, J. A; *Energy Simulation..,* P162.

[5]    ibid. Clarke, J. A; *Energy Simulation..,* P162.

[6]    ibid. Clarke, J. A; *Energy Simulation..,* P162.

[7]    ibid. Clarke, J. A; *Energy Simulation..,* P162.

[8]    Kreider, J. F; Kreith, F; *Solar Energy Handbook*, McGraw- Hill Book Company, New York, 1981, P2-10.

[9]    Perez, R; Ineichen, R; Zelenka, A; "Making Full Use of the Clearness Index for Parameterizing Hourly Insolation Conditions." *Solar Energy,* Vol. 45, No. 2, 1990, P111- 114.

[10]    Rapp, D; *Solar Energy*, Prentice- Hall inc., Englewood Cliffs, N.J; 1981, P53

[11]    ibid. Clarke, J. A; *Energy Simulation..,* P224.

[12]    ibid. Clarke, J. A; *Energy Simulation..,* P229.

[13]    ibid. Page, Prof. J et al, *Climate in the UK...,* P337.

[14]    ibid. Page, Prof. J et al, *Climate in the UK...,*349.

[15]    Grenier, J. C; De La Casiniere, A; Cabot, T; "A Spectral Model of Linke's Turbidity Factor and its Experimental Implications." *Solar Energy*, Vol. 52, No. 4, 1994, P311.

[16]    ibid. Clarke, J. A; *Energy Simulation..,* P229.

[17]    ibid. Clarke, J. A; *Energy Simulation..,* P227.

[18]    ibid. Clarke, J. A; *Energy Simulation..,* P229.

[19]    Szokolay, S. V; *World Solar Architecture*, The Architectural Press, London, 1980, P233.

[20]   ibid. Szokolay, S. V; *World Solar Architecture*, P233.

[21]   ibid. Kreider, J. F; Kreith, F; *Solar Energy Handbook*, P 2-68.

[22]   ibid. Clarke, J. A; *Energy Simulation..*, P164.

[23]   ibid. Page, Prof. J et al, *Climate in the UK...,* P357.

[24]   ibid. Page, Prof. J et al, *Climate in the UK...,* P357.

[25]   ibid. Page, Prof. J et al, *Climate in the UK...,* P358.

[26]   ibid. Page, Prof. J et al, *Climate in the UK...,* P357.

[27]   ibid. Page, Prof. J et al, *Climate in the UK...,* P358.

[28]   ibid. Page, Prof. J et al, *Climate in the UK...,* P365- 367.

[29]   ibid. Clarke, J. A; *Energy Simulation..*, P216.

[30]   ibid. Clarke, J. A; *Energy Simulation..*, P215.

[31]   van Straaten, J. F; *Thermal Performance of Buildings*, Elsevier Publishing Company, London, 1967, P9.

[32]   ibid. van Straaten, J. F; *Thermal Performance...,* P9.

[33]   ibid. Clarke, J. A; *Energy Simulation..*; P220- 221.

[34]   McAdams, W.H; *Heat Transmission*, McGraw- Hill, New York, 1954.

[35]   Alamandri, F; Hammond, G. P; "Improved data correlations for buoyancy- driven convection in rooms." *Building Services Engineering Research and Technology*, Vol. 4, No. 3, 1983, P107.

[36]   ibid. Alamandri, F; Hammond, G. P; *Building Services Engineering...,*  P107.

[37]   ibid. Alamandri, F; Hammond, G. P; *Building Services Engineering...,* P110.

[38]   ibid. Alamandri, F; Hammond, G. P; *Building Services Engineering...,* P108.

[39]   Fishendem, M; *The Calculation of Heat Transmission*; HMSO, London, 1932, P119.

[40]   ibid. Clarke, J. A; *Energy Simulation..*, P198.

[41]   ibid. Clarke, J. A; *Energy Simulation..*, P199.

[42]   ibid. Kreider, J. F; Kreith, F; *Solar Energy Handbook*, P4-38.

[43]   ibid. Kreider, J. F; Kreith, F; *Solar Energy Handbook*, P4-38.